HHS Public Access

Author manuscript

Biomaterials. Author manuscript; available in PMC 2015 May 12.

Published in final edited form as:

Biomaterials. 2010 March ; 31(7): 1765–1772. doi:10.1016/j.biomaterials.2009.11.038.

Polymeric micelles for the pH-dependent controlled, continuous low dose release of paclitaxel

Adam WG. Alani[1], **Younsoo Bae**[2], **Deepa A. Rao**[3], and **Glen S. Kwon**[1,*]

[1]Pharmaceutical Sciences Division, School of Pharmacy, University of Wisconsin, 777 Highland Ave, Madison, WI 53705, USA

[2]Department of Pharmaceutical Sciences, College of Pharmacy, University of Kentucky, 725 Rose Street, Lexington, KY 40536, USA

[3]Department of Pharmaceutical, Biomedical and Administrative Sciences, College of Pharmacy & Health Sciences, Drake University, 2507 University Ave, Des Moines, IA 50311, USA

Abstract

Poly(ethylene glycol)-block-poly(aspartate-hydrazide) (PEG-p(Asp-Hyd)) was modified using either levulinic acid (LEV) or 4-acetyl benzoic acid (4AB) attached via hydrazone bonds. Paclitaxel (PTX) conjugated to the linkers formed PEG-p(Asp-Hyd-LEV-PTX) and PEG-p(Asp-Hyd-4AB-PTX). PEG-p(Asp-Hyd-LEV-PTX) and PEG-p(Asp-Hyd-4AB-PTX) assemble into unimodal polymeric micelles with diameters of 42 nm and 137 nm, respectively. PEG-p(Asp-Hyd-LEV-PTX) and PEG-p(Asp-Hyd-4AB-PTX) at a 1:1 and 1:5 molar ratio assemble into unimodal mixed polymeric micelles with diameters of 85 and 113 nm, respectively. PEG-p(Asp-Hyd-LEV-PTX) micelles release LEV-PTX faster at pH 5.0 than at pH 7.4 over 24 hr. At pH 7.4 mixed polymeric micelles at 1:5 ratio show no difference in LEV-PTX release from PEG-p(Asp-Hyd-LEV-PTX) micelles. Mixed polymeric micelles at 1:5 molar ratio gradually releases LEV-PTX at pH 5.0, with no release of 4AB-PTX. PEG-p(Asp-Hyd-LEV-PTX) micelles and mixed polymeric micelles exert comparable cytotoxicity against SK-OV-3 and MCF-7 cancer cell lines. In summary, mixed polymeric micelles based on PEG-p(Asp-Hyd-LEV-PTX) and PEG-p(Asp-Hyd-4AB-PTX) offer prospects for pH-dependent release of PTX, offering a novel pro-drug strategy for adjusting its pharmacokinetic and pharmacodynamic properties for cancer therapy. If successful this delivery system offers an alternative new mode of delivery for paclitaxel with a new scope for its efficacy along with a minimal synthetic framework needed to accomplish this.

1. Introduction

Paclitaxel is one of the most broadly active compounds available for the treatment of human malignancy, with activity demonstrated in cancers of the ovary, breast, lung, head and neck, esophagus, bladder, testis, endometrium, and possibly hematological and pediatric malignancies [1]. PTX is also a strong inhibitor of the endothelial cell function relevant to angiogenesis at low concentrations [2–3]. New research has shown that PTX has anti-angiogenic activity by inhibiting vascular endothelial-cell proliferation, motility and cord/

*Corresponding author: Tel.: +1 608 265 5183; fax: +1 608 262 5345. gskwon@pharmacy.wisc.edu (G.S. Kwon).

tube formation at extremely low concentrations (e.g., picomolar) [3–4]. The anti-angiogenic efficacy of PTX seems to be amplified by administering comparatively low doses of PTX [5]. Due to the low aqueous solubility of PTX, 0.3 μM [6], it is commercially available as Taxol® in a vehicle composed of 1:1 of Cremophor EL® (CrEL) (polyoxyethylated castor oil) and ethanol. Side effects caused by CrEL include hypersensitivity reactions, nephrotoxicity, and neurotoxicity [7–9]. Further, CrEL at clinically relevant concentrations nullifies the anti-angiogenic activity of paclitaxel [3]. Taxol® is also limited by its short term physical stability upon dilution as PTX tends to precipitate out of the aqueous media [10]. Other problems associated with ethanol and CrEL include leaching of plasticizer from polyvinyl chloride infusion bags and sets [11]. Thus, there are many strategies for improved vehicles for the delivery of PTX with high anti-tumor and anti-angiogenic activity with reduced formulation related adverse effects, culminating in the recent approval of Abraxane®, albumin nanoparticles that permit higher doses of PTX over Taxol®, owing to an absence of CrEL [12].

Amphiphilic block copolymers (ABCs) assemble into polymeric micelles that are nanoscopic, have a core/shell architecture, and have wide potential in cancer therapy for the tumor targeting of PTX by the enhanced permeability and retention (EPR) effect [13]. Poly(ethylene glycol)-*block*-poly(β-benzyl L-aspartate) (PEG-PBLA) is an ABC that has been used as a starting point for polymeric micelles for the delivery of chemotherapy [14–15]. A major advantage of PEG–PBLA is its ease in side chain chemistry, allowing side chain variation for drug solubilization and/or pro-drug design. The replacement of benzyl ester protecting groups on PEG-PBLA with 4-phenyl-1-butanol leads to polymeric micelles that increase the water solubility of PTX to ca. 10 mg/mL, increase its plasma half-life from ca. 1 to 6 hr in mice, and increase PTX levels in solid tumors by the EPR effect [16]. NK105 is in Phase II clinical trials for stomach cancer therapy [16]. Recent research on doxorubicin (DOX) outlines an alternative prodrug strategy for PTX: replacement of benzyl groups on PEG-PBLA with hydrazine permits the coupling of DOX via hydrazone linkages (PEG-p(Asp-Hyd-DOX)). PEG-p(Asp-Hyd-DOX) micelles are stable at pH 7.4 and release DOX under acidic conditions, associated with the extracellular environment in hypoxic solid tumors and endosomal/lysosomal pathway of cells [17–20]. However, PTX lacks an aldehyde or ketone group for a hydrazone linkage, mandating a linker for pH-sensitive release.

The goal of this proposed research is to prepare polymeric micelles that can solubilize PTX and release this anti-cancer agent in a pH-dependent manner. In addition, these polymeric micelles will provide a formulation platform that can be tailored for specific regimens for PTX administration to maximize its anti-angiogenic activity, which is based on administering comparatively low doses of PTX. Taking a hydrazone prodrug strategy, we proposed coupling an aliphatic linker, levulinic acid (LEV) or an aromatic linker, 4-acetyl benzoic acid (4-AB), on poly(ethylene glycol)-*block*-poly(aspartate-hydrazide) (PEG-p(Asp-Hyd)) to introduce carboxylic acid groups for attachment of PTX by an ester bond. Following the synthesis we expect these polymers to self-assemble into micelles that will release PTX in a pH-dependent manner. PEG-p(Asp-Hyd-LEV-PTX) and PEG-p(Asp-Hyd-4AB-PTX) will also be used to form mixed micelles and determine PTX pH-dependent

release profiles from these micelles. We have hypothesized that mixed polymeric micelles composed of PEG-p(Asp-Hyd-LEV-PTX) and PEG-p(Asp-Hyd-4AB-PTX) would have a composite release profile for PTX, reflecting the rate of hydrazone hydrolysis of LEV-PTX and 4AB-PTX in mixed polymeric micelles (Fig. 1). If successful, we anticipate that these polymeric micellar delivery system offer new prospects for moderating the pH-dependent release of PTX and for enhancing its pharmacokinetic and pharmacodynamic properties, aiming for advances in cancer therapy for solid tumors.

2. Materials & Methods

2.1. Materials

α-methoxy-ω-amino-poly(ethylene glycol) (PEG-NH_2) (M_n 12,000 g/mol, PDI = 1.03) was purchased from NOF Corporation (Tokyo, Japan). PTX was obtained from LKT laboratories Inc (St. Paul, MN). SK-OV-3 (Human Caucasian ovary adenocarcinoma) and MCF-7 cell lines (Human breast adenocarcinoma) were purchased from American Type Culture Collection (Manassas, VA). All other materials and reagents were obtained from Sigma-Aldrich Inc (Milwaukee, WI) or Fisher Scientific Inc (Fairlawn, NJ).

2.2. Methods

2.2.1 Synthesis of amphiphilic diblock copolymer PEG-PBLA—PEG-PBLA was synthesized as previously reported [21–22]. Briefly, β-benzyl-L-aspartate *N*-carboxyanhydride (BLA-NCA) was prepared using Fuchs-Farthing method, triphosgene 5.76 g (19.4 mmol) was added to 10 g (44.8 mmol) of β-benzyl-L-aspartate in dry tetrahydrofuran (THF) (150 mL), and the reaction was allowed to proceed at 40 °C until the solution became clear. BLA-NCA was purified by recrystallization from hexane and purity was confirmed by measuring its melting point at 129.5 °C. Ring opening polymerization of BLA-NCA (1.7 g, 6.82 mmol) was initiated from the terminal primary amine group of PEG-NH_2 (2.0 g, 0.16 mmol). The polymerization was carried out under argon atmosphere in anhydrous DMSO (7.0 mL) at 40°C for 2 days. PEG-PBLA was obtained after precipitation from diethyl ether followed by freeze drying from benzene.

2.2.2 Synthesis of PEG-p(Asp-Hyd)—PEG-p(Asp-Hyd) was synthesized as previously reported [17–18, 20]. Briefly, PEG-PBLA (1.0 g, 0.05 mmol) was dissolved in anhydrous N,N-dimethylformamide (DMF) (10 mL), and anhydrous hydrazine (1.2 eq with respect to benzyl groups) was added to the polymer solution under argon atmosphere. The reaction was allowed to proceed at 40 °C for 1 hr followed by polymer precipitation in diethyl ether. PEG-p(Asp-Hyd) was dialyzed against 0.25% ammonia solution then 0.025% ammonia solution and freeze-dried to obtain the product, PEG-poly(Asp-Hyd). The structure of PEG-poly(Asp-Hyd) was confirmed using ^{1}H NMR (500MHz, DMSO-d_6).

2.2.3 Synthesis of PEG-p(Asp-Hyd-LEV) and PEG-p(Asp-Hyd-4AB)—The pH labile hydrazone bond was formed via the reaction of the hydrazine groups on the PEG-p(Asp-Hyd) with the ketone group on LEV or 4AB, resulting in the formation of PEG-p(Asp-Hyd-LEV) or PEG-p(Asp-Hyd-4AB), respectively. PEG-p(Asp-Hyd) (750 mg, 0.046 mmol) was dissolved in 15 mL anhydrous dimethyl sulfoxide (DMSO). 4AB or LEV (1.2 eq

with respect to hydrazide group) was dissolved in anhydrous DMSO and added to the polymer solution under argon. The reaction was allowed to proceed for 48 hr at 45 °C. PEG-p(Asp-Hyd-LEV) or PEG-p(Asp-Hyd-4AB) was collected from diethyl ether, solubilized in DMF, and dialyzed against DMF using regenerated cellulose (MWCO: 3,000 g/mol). Polymers were collected from diethyl ether and then freeze dried from benzene.

2.2.4. Synthesis of PEG-p(Asp-Hyd-LEV-PTX) and PEG-p(Asp-Hyd-4AB-PTX)— PEG-p(Asp-Hyd-LEV) (200 mg, LEV = 0.376 mmol) or PEG-p(Asp-Hyd-4AB) (200 mg, 4AB = 0.352 mmol) was conjugated to PTX (600 mg, 0.468 mmol) using N,N′-diisopropylcarbodiimide (DIC; 56 mg, 0.44 mmol) as coupling agent in the presence of 4-dimethylaminopyridine (DMAP; 21.7 mg, 0.17 mmol). The reaction was carried out in (dichloromethane (DCM): DMF) (5:1) (7.0 mL) at 25 °C for 48 hr. PEG-p(Asp-Hyd-LEV-PTX) or PEG-p(Asp-Hyd-4AB-PTX) was collected by evaporating DCM, and the residue was diluted in 5.0 mL DMF. The polymer solution was dialyzed against 1.0 L DMF (DMF was changed 3 times) using regenerated cellulose (MWCO: 6–8000 g/mol). The polymer was precipitated in diethyl ether, freeze-dried from benzene, and the product was collected as a white powder. The structure and the degree of substitution of PTX on PEG-p(Asp-Hyd-LEV-PTX) or PEG-p(Asp-Hyd-4AB-PTX) was confirmed by ^{1}H NMR (500MHz, DMSO-d_6), and their purity was confirmed by reverse-phase HPLC.

2.2.5. Synthesis of LEV-PTX and 4AB-PTX—PTX 200 mg (0.23 mmol) was dissolved in 15 mL anhydrous THF. Separately, DIC (46 mg, 0.36 mmol), DMAP (18 mg, 0.15 mmol) and LEV (34 gm, 0.30 mmol) or 4AB (48 mg, 0.3 mmol) were dissolved in 10 mL anhydrous THF. The mixture was stirred for 45 min and then added to the PTX solution. The reaction was run for 3 hr with stirring at room temperature. The solvent was removed under vacuum. The residue was dissolved in DCM and transferred into separation funnel and washed three times with saturated sodium chloride solution. After washing, the organic layer was collected and DCM was removed by vacuum. The residue was dissolved in Acetonitrile (ACN): Water (3:2) and purified through reverse-phase chromatography column (derivatized silica gel octyl (C_8) Zorbax LP 100/40 C_8). The structure of LEV-PTX and 4AB-PTX was confirmed by ^{1}H NMR, ^{13}C NMR and, 2D HSQC (Heteronuclear Single Quantum Coherence) and reverse-phase HPLC (500MHz, DMSO-d_6) (Fig. 2) and its purity confirmed by reverse-phase HPLC section (2.2.6).

LEV-PTX: ^{1}H NMR 500 MHz (DMSO-d_6) data: δ=9.21 (d, 1H, N), 7.96/7.61/ 7.59 (5H, arom.: O–Bz), 7.87/7.46/7.54 (5H, arom.: N–Bz), 7.44/7.21 (5H, arom: Ph3′-), 6.28 (s, 1H, 10-), 5.91 (t, 1H, 13-), 5.43. (dd, 1H, 3′-), 5.43 (d, 1H, 2-), 4.70 (s, 1H, 1-O), not observed (s, 1H, 7-O), 4.93 (dd, 1H, 5-), 4.61 (d, 1H, 2′-), 4.12 (dd, 1H, 7-), 4.11/4.10 (dd, 2H, 20α-/20β-), 3.60 (d, 1H, 3-), 3.34 (s, 3H, 10-OCOC), **2.37(t, 2H 3″-)**, **2.65 (t, 2H, 2″-)**, 2.31 (m, 1H, 6α-), 2.11 (s, 3H, 4-OCOC), **2.11 (s, 3H, 5″-)**,1.65./1.92 (m, 2H, 14-), 1.80 (s, 3H, 18-), 1.75 (m, 1H, 6β-), 1.52 (s, 3H, 19-), 1.04 (s, 3H, 16-), 1.01 (s, 3H, 17-). **^{13}C NMR**: (125.6 MHz, DMSO-d_6): δ=207.09 (C-9), **206.24 (C-1″)**, 172.74 (C-1′), **171.75 (C-4″)**, 169.64 (10-O), 169.10 (4-O), 166.34 (3′-NH), 165.22 (2-O), 139.24 (C-12), 133.36 (C-11), 134.49/134.22/ 131.32/129.98/129.56/128.68/128.32/128.26/127.66/127.43/127.39 (C-arom) 83.60 (C-5), 80.26 (C-4), 76.76 (C-1), 76.17 (C-20), 75.36(C-7), 74.78 (C-10), 74.49

(C-2), 73.62 (C-2′), 70.47 (C-13), 57.42 (C-8), 53.96 (C-3′), 45.19 (C-3), 42.38 (C-15), **37.51 (C-3″)**, 36.54 (C-6), 34.68 (C-14), **29.31 (C-5″)**, **27.35 (C-2″)**, 26.32 (C-16), 22.55 (C-17), 21.66 (10-OCO), 20.26 (4-OCO), 13.85 (C-18), 9.77 (C-19).

4AB-PTX: ^{1}H NMR 500 MHz (DMSO-d_6) data: δ=8.91 (d, 1H, N), **8.02/8.03 (4H, arom: 3″-/4″-)**, 7.96/7.71/ 7.61 (5H, arom.: O–Bz), 7.87/7.52/7.48 (5H, arom.: N–Bz), 7.39/7.21 (5H, arom: Ph3′-), 6.29 (s, 1H, 10-), 5.87 (t, 1H, 13-), 5.40. (dd, 1H, 3′-), 4.51 (d, 1H, 2′-), 5.43 (d, 1H, 2-), 4.70 (s, 1H, 1-O), not observed (s, 1H, 7-O), 4.91 (dd, 1H, 5-), 4.05 (dd, 1H, 7-), 4.11/4.10 (dd, 2H, 20α-/20β-), 3.60 (d, 1H, 3-), **2.65 (s, 3H, 7″-),** 2.31 (m, 1H, 6α-), 2.10 (s, 3H, 4-OCOC), 1.60./1.90 (m, 2H, 14-), 3.63 (s, 3H, 10-OCOC), 1.79 (s, 3H, 18-), 1.70 (m, 1H, 6β-), 1.51 (s, 3H, 19-), 1.02 (s, 3H, 16-), 1.04 (s, 3H, 17-). **^{13}C NMR** (125.6 MHz, DMSO-d_6): δ=202.37 (C-9), **197.71 (C-1″)**, 172.73 (C-1′), 169.85 (10-O), 168.76 (4-O), 166.23 (3′-NH), 165.18 (2-O), **167.56 (C-6″)**, 139.24 (C-12), **137.99 (C-5″)**, 133.43 (C-11), 134.47/133.34/ 131.33/129.96/129.55/128.69/128.27 /127.45/127.38 (C-arom.) 83.58 (C-5), 80.24 (C-4), 76.74 (C-1), 76.44 (C-20), 75.05(C-7), 74.76 (C-10), 74.49 (C-2), 73.61 (C-2′), 69.72 (C-13), 57.41 (C-8), 56.33 (C-3′), 46.09 (C-3), 42.96 (C-15), 36.55 (C-6), 34.68 (C-14), **27.39 (C-7″)**, 26.30 (C-16), 20.67 (4-OCO), 22.14 (C-17), 21.29 (10-OCO), 13.81 (C-18), 9.76 (C-19).

2.2.6. Reverse-phase HPLC—A 20 μL sample of PTX, LEV-PTX, 4AB-PTX, PEG-p(Asp-Hyd-LEV-PTX) or PEG-p(Asp-Hyd-4AB-PTX) in ACN at 2.5 mg/mL was injected into a Zorbax SB-C8 Rapid Resolution cartridge (4.6×75mm, 3.5 micron, Agilent). In addition, a 400 μL sample of PEG-p(Asp-Hyd-4AB-PAX) or PEG-p(Asp-Hyd-LEV-PAX) in ACN at 2.5 mg/ml was incubated in 150 μL double distilled (DD) H_2O and 50 μL 6 N HCl for 1 hr to ensure the complete release of LEV-PTX or 4AB-PTX, attached onto PEG-p(Asp-Hyd-LEV-PTX) or PEG-p(Asp-Hyd-4AB-PTX). This sample was centrifuged for 3 min at 10,000 rpm, filtered with 0.45 μm nylon filter, and 20 μL was injected into a Zorbax SB-C8 Rapid Resolution cartridge (4.6×75mm, 3.5 micron, Agilent). For all samples, the mobile phase was an isocratic mixture of 47% ACN and 53% aqueous phase containing 0.1% phosphoric acid and 1% methanol in DD H_2O, and the column temperature was 40 °C. The HPLC system was a Shimadzu prominence HPLC system (Shimadzu, JP), consisting of a LC-20AT pump, SIL-20AC HT autosampler, CTO-20AC column oven and a SPD-M20A diode array detector.

2.2.7. NMR spectroscopy—NMR measurements were performed on $^{\text{UNITY}}$*INOVA* NMR spectrometers (Varian, USA) model operating at 500 MHz normal proton frequencies. Sample temperature was regulated for all measurements and was set at 80 °C. The spectrometer was equipped with FTS Systems preconditioning device (composed of refrigerating unit, internal temperature controller and inclusion transfer line). Acquisition parameters were adjusted on a case-by-case basis to provide adequate signal-to-noise and spectral resolution, the latter typically at 0.5 and 4.2 ppB/point for 1D high-resolution ^{1}H and ^{13}C spectra, respectively. Carbon-13 spectra were acquired with proton decoupling. All ^{1}H and ^{13}C spectra were referenced with respect to TMS at 0.0 ppm.

2.2.8. Preparation and characterization of PEG-p(Asp-Hyd-LEV-PTX) and PEG-p(Asp-Hyd-4AB-PTX) micelles and their mixed polymeric micelles—PEG-p(Asp-Hyd-LEV-PTX) or PEG-p(Asp-Hyd-4AB-PTX) (12 mg) was dissolved in 1.0 mL of ACN and mixed with 3.0 mL of double-distilled (DD) H_2O. ACN was removed under vacuum at 60 °C, and the volume was reduced to 1.0 mL, followed by the addition of fresh 3.0 mL DD H_2O. This process of evaporation and dilution with DD H_2O was repeated three times to ensure complete removal of ACN. In the last step, the final volume was adjusted with 10 mM buffer (acetate buffer at pH 5.0 or phosphate buffer at pH 7.4) [23] to obtain a final concentration of 2.5 mg/mL of the polymer. The 2.5 mg/mL of the polymer corresponds to 0.20 mmol/mL of LEV-PTX in PEG-p(Asp-Hyd-LEV-PTX) or to 1.0 mmol/mL of 4AB-PTX in PEG-p(Asp-Hyd-4AB-PTX). The micellar solution was filtered using a 0.45 μm filter, and the polymeric micelle size was characterized by dynamic light scattering (DLS). A ZETASIZER Nano-ZS (Malvern Instruments Inc., UK) equipped with He-Ne laser (4mW, 633 nm) light source and 173° angle scattered light collection configuration was used to determine polymeric micelle mean diameters. The hydrodynamic diameter of polymeric micelles was calculated based on the Stokes-Einstein equation. Correlation function was curve-fitted by cumulant method to calculate mean size and polydispersion index (PDI). All measurements were repeated three times, and volume-weighted particle sizes are presented as the average diameter with standard deviation. Mixed polymeric micelles were prepared by dissolving a fixed molar ratio of PEG-p(Asp-Hyd-LEV-PTX) with PEG-p(Asp-Hyd-4AB-PTX) in 1.0 mL ACN, followed by assembly as described above. The molar ratio of PEG-p(Asp-Hyd-LEV-PTX) and PEG-p(Asp-Hyd-4AB-PTX) was calculated according to the number of moles of LEV-PTX per weight of PEG-p(Asp-Hyd-LEV-PTX) relative to the number of moles of 4AB-PTX per weight of PEG-p(Asp-Hyd-4AB-PTX). Mixed polymeric micelles were prepared at 1:1 and 1:5 molar ratios, corresponding to PEG-p(Asp-Hyd-LEV-PTX) (2.5 mg/mL, 0.2 mmol/mL LEV-PTX) with PEG-p(Asp-Hyd-4AB-PTX) (0.5 mg/mL, 0.20 mmol/mL 4AB-PTX), and PEG-p(Asp-Hyd-LEV-PTX) (2.5 mg/mL, 0.2 mmol/mL LEV-PTX) with PEG-p(Asp-Hyd-4AB-PTX) (2.5 mg/mL, 1.0 mmol/mL 4AB-PTX), respectively.

2.2.9. In vitro drug release experiments—PEG-p(Asp-Hyd-LEV-PTX) and PEG-p(Asp-Hyd-4AB-PTX) micelles were prepared as described above (section 2.2.8), and a sample of 2.5 mL was loaded into a Slide-A-Lyzer® (Thermo Scientific Inc.) dialysis 3.0 mL cassette with a MWCO of 20,000 g/mol. Four cassettes was used in each experiment (n = 4). The cassettes were placed in 2.5 L of 10 mM buffer (acetate buffer at pH 5.0 or phosphate buffer at pH 7.4) [23], which was changed every 3 hr to ensure sink conditions. The sampling time intervals were 0, 0.5, 1, 2, 3, 6, 9, 12, 24 hr. A sample of 150 μL at each time point was withdrawn, and the cassette was replenished with fresh 150 μL of buffer. The sample was incubated in 400 μL ACN and 50 μL 6N HCl for 1hr to ensure the full release of the LEV-PTX or 4AB-PTX attached to the polymer chain. Samples were analyzed by reverse-phase HPLC for drug content (section 2.2.6).

2.2.10. In vitro cytotoxicity experiments—The CellTiter-Blue® cell viability assay (Promega, Madison, WI) was used to determine the cytotoxicity for MCF-7 and SK-OV-3 cell lines. In a 96 well culture plate, MCF-7 or SK-OV-3 cells were seeded at an initial

density of 2500 and 3500 cells/well respectively in 100 μL of RPMI 1640 supplemented with 10 % fetal bovine serum (FBS), 100 IU penicillin, and 100 μg/ mL streptomycin, and 2 mM L-glutamine. The seeded cells were incubated at 37 °C in 5% CO_2 atmosphere for 12 hr. On the day of the experiment, PTX, LEV or 4AB-PTX was dissolved in DMSO while, individual or mixed polymeric micelles (section 2.2.8) were diluted in PBS. Each compound or polymeric micelle formulation was diluted into the wells to yield PTX, LEV-PTX and/or 4AB-PTX concentration of 0.01, 0.1, 1, 5, 10, 50, 100, 500, 1000, and 10000 nM. Cells were also treated with PEG-p(Asp-Hyd-LEV) or PEG-p(Asp-Hyd-4AB) directly dissolved in PBS to evaluate the toxicity of polymers without PTX. Additional cells were treated with DMSO diluted in medium or medium only as controls. Treated and control cells were incubatedfor 72 hr at 37 °C in 5% CO_2 atmosphere. Thereafter plates were removed from incubator and 20 μL of the CellTiter-Blue® reagent was added to each well and the plate were incubated for 2 hr at 37 °C in 5% CO_2 atmosphere. After incubation fluorescence was recorded at ($560_{EX}/590_{EM}$). Cell viability was calculated as the percentage of the fluorescence intensity of the treated cells divided by the fluorescence intensity of control cells multiplied by 100. The IC_{50} values were determined by using log(inhibitor) vs. response (variable slope) equation using GraphPad Prism version 5.00 for Windows, GraphPad Software, San Diego California USA, www.graphpad.com.

2.2.11. Data analysis—Statistical analysis was performed using one-way ANOVA at 5 % significance level combined with Tukey's Multiple Comparison Test or t-test at 5 % significance level. IC_{50} was calculated by fitting the data to log(inhibitor) vs. response (variable slope) equation. All data analyses were performed using GraphPad Prism version 5.00 for Windows, GraphPad Software, San Diego California USA, www.graphpad.com.

3. Results

3.1. Synthesis of PEG-p(Asp-Hyd-LEV-PTX) and PEG-p(Asp-Hyd-4AB-PTX)

PEG-PBLA (**3**) was synthesized by the polymerization of BLA-NCA (**1**) using PEG-NH_2 (**2)** as macro-initiator (Fig. 3). The structure of PEG-PBLA was confirmed by ^{1}H NMR (data not shown). The number of β-benzyl-L-aspartate units on PEG-PBLA was 40. The molecular weight and the polydispersity index of PEG-PBLA were 20,400 g/mol and 1.10, respectively, by gel permeation chromatography, using PEG molecular weight standards (Scientific Polymer Products Inc. Ontario, NY). PEG-p(Asp-Hyd) (**4**) was synthesized by an ester-amide exchange reaction, and its structure was confirmed by ^{1}H NMR (500MHz, DMSO-d_6) (data not shown).

PEG-p(Asp-Hyd-LEV) or PEG-p(Asp-Hyd-4AB) (**5)** (Fig. 3) were synthesized by hydrazone bond formation between the hydrazide groups on PEG-p(Asp-Hyd) (**4**) and the ketone group on LEV or 4AB. The number of LEV on PEG-p(Asp-Hyd-LEV-PTX) was calculated from the peak ratio of methylene protons of PEG (-$\boldsymbol{OCH_2CH_2}$- : δ 3.5 ppm) (resonance **a**) relative to methyl protons of LEV (-$\boldsymbol{CH_3}$- : δ 1.86 ppm) (resonance **b**) (Fig. 4A). The number of LEV on PEG-p(Asp-Hyd-LEV-PTX) was 40, corresponding to a 100% substitution. The number of 4AB on PEG-p(Asp-Hyd-4AB) was calculated from the peak ratio of the methylene protons of PEG (-$\boldsymbol{OCH_2CH_2}$- : δ 3.5 ppm) (resonance **a**) relative to phenyl protons of 4AB (-$\boldsymbol{C_6H_5}$: δ 7.8 ppm) (resonance **b) (**Fig. 4B). The number of 4AB

attached on PEG-p(Asp-Hyd-4AB-PTX) was 40, again corresponding to a 100% substitution.

PEG-p(Asp-Hyd-LEV-PTX) and PEG-p(Asp-Hyd-4AB-PTX) (**6)** (Fig. 3) were synthesized by conjugation of PTX via an ester bond on PEG-p(Asp-Hyd-LEV) or PEG-(p(Asp-Hyd-4AB). The structures of both polymers were confirmed by ^{1}H NMR (500MHz, DMSO-d_6) (Figs 5A and 5B). The number of PTX molecules attached onto PEG-p(Asp-Hyd-LEV-PTX) and PEG-p(Asp-Hyd-4AB-PTX) was 15, calculated from the peak ratio of the methylene protons of PEG ***(-OCH$_2$CH$_2$-*** : δ 3.5 ppm) (resonance **a**) relative to PTX methyl protons (6H ***-CH$_3$-*** : δ 1.1 ppm) (resonance **b**) (Fig. 5A), corresponding to a 37.5% degree of drug substitution, whereas the number of PTX molecules attached onto PEG-p(Asp-Hyd-4AB-PTX) was 35 from the peak ratio of the methylene protons of PEG (***-OCH$_2$CH$_2$***-: δ 3.5 ppm) (resonance **a**) to PTX methyl protons (6H ***-CH$_3$-*** : δ 0.7 ppm) (resonance **b**) (Fig. 5B), corresponding to a 87.5% degree of drug substitution. The absence of un-reacted PTX was confirmed by reverse-phase HPLC: PEG-p(Asp-Hyd-LEV-PTX) eluted at 1.30 min, whereas PEG-p(Asp-Hyd-4AB-PTX) eluted at 1.40 min, both detected at λ_{max} 227 nm as single peaks, without evidence of PTX, which elutes at 3.3 min. PEG-p(Asp-Hyd-LEV-PTX) hydrolyzed with HCl displayed a single peak at 4.4 min, corresponding to LEV-PTX, whereas PEG-p(Asp-Hyd-4AB-PTX) showed a single peak at 6.3 min corresponding to free 4AB-PTX. In both cases, PTX due to ester hydrolysis of LEV-PTX or 4AB-PTX was not detected. Based on reverse-phase HPLC, the levels of LEV-PTX on PEG-p(Asp-Hyd-LEV-PTX) weight and 4AB-PTX on PEG-p(Asp-Hyd-4AB-PTX) were 0.08 and 0.4 mmol/mg, respectively.

3.2. DLS measurements on PEG-p(Asp-Hyd-LEV-PTX) and PEG-p(Asp-Hyd-4AB-PTX) micelles and their mixed polymeric micelles

The average hydrodynamic diameters of PEG-p(Asp-Hyd-LEV-PTX) and PEG-p(Asp-Hyd-4AB-PTX) micelles were 41.9 ± 0.6 and 137.0 ± 2.4 nm, respectively (Fig. 6). The average hydrodynamic diameter for their mixed polymeric micelles at a 1:1 molar ratio was 85.53 ± 0.14 nm, whereas the average hydrodynamic diameter for the mixed polymeric micelles at a 1:5 molar ratio was 113.40 ± 0.93 nm (Fig. 6). PEG-p(Asp-Hyd-LEV-PTX) and PEG-p(Asp-Hyd-4AB-PTX) micelles were all unimodal in size distribution. The effect of buffer pH was evaluated by preparing PEG-p(Asp-Hyd-LEV-PTX) and PEG-p(Asp-Hyd-4AB-PTX) micelles at pH 5.0 and 7.4, and buffer pH did not influence the dimensions of any PEG-p(Asp-Hyd-LEV-PTX) and PEG-p(Asp-4AB-PTX) micelles (data not shown).

3.3. In vitro drug release experiments on PEG-p(Asp-Hyd-LEV-PTX) and PEG-p(Asp-Hyd-4AB-PTX) micelles and their mixed polymeric micelles

The release of LEV-PTX and 4AB-PTX from PEG-p(Asp-Hyd-LEV-PTX) or PEG-p(Asp-Hyd-4AB-PTX) micelles were evaluated at pH 5.0 and 7.4 over 24 hr by a simple dialysis method. PEG-p(Asp-Hyd-LEV-PTX) micelles gradually released LEV-PTX over the course of the study without a burst effect (Figs 7A and 7B). The percentages of LEV-PTX released from PEG-p(Asp-Hyd-LEV-PTX) after 24 hr at pH 5.0 and 7.4 were 57.6 ± 1.9 % and 29.2 ± 5.1%, respectively. The release data showed that LEV-PTX release is statistically significantly higher at pH 5.0 than pH 7.4 (Fig 7A &7B). On the other hand, no 4AB-PTX

was released from PEG-p(Asp-Hyd-4AB-PTX) micelles at pH 5.0 or 7.4 over the course of 24 hr (data not shown).

The release profiles of LEV-PTX from the mixed polymeric micelles at 1:1 and 1:5 molar ratios at pH 5.0 and 7.4 are shown in Figs 7A and 7B. Mirroring PEG-p(Asp-Hyd-LEV-PTX) micelles, mixed polymeric micelles gradually released LEV-PTX without a burst effect. At a 1:1 molar ratio, the percentage of LEV-PTX released after 24 hr at pH 5.0 was 44.9 ± 1.0 %, whereas it was 34.0 ± 1.1% at pH 7.4. At a 1:5 molar ratio, the percentages of LEV-PTX released after 24 hr at pH 5.0 and pH 7.4 were 28.0 ± 5.8 % and 19.0 ± 6.9%, respectively. At pH 5.0, no statistically significant difference was noticed between the release profiles of LEV-PTX from PEG-p(Asp-Hyd-LEV-PTX) micelles and mixed polymeric micelles at a 1:1 ratio (Fig. 7A). However, the release profiles of LEV-PTX from mixed polymeric micelles at a 1:5 ratio at pH 5.0 was statistically significantly lower than its release from the PEG-p(Asp-Hyd-LEV-PTX) micelles or mixed polymeric micelles at a 1:1 ratio (Fig. 7A). At pH 7.4, no significant difference was noticed among the release profiles of LEV-PTX from all polymeric micelles (Fig. 7B). Mixed polymeric micelles composed of PEG-p(Asp-Hyd-LEV-PTX):PEG-p(Asp-Hyd-4AB-PTX) at 1:1 and 1:5 molar ratios at pH 5.0 and 7.4 did not release 4AB-PTX as determined by reverse-phase HPLC.

3.4. In vitro cytotoxicity experiments on PEG-p(Asp-Hyd-LEV-PTX) and PEG-p(Asp-Hyd-4AB-PTX) micelles and their mixed polymeric micelles

IC_{50} values of PTX, LEV-PTX, 4AB-PTX, PEG-p(Asp-Hyd-LEV-PTX) micelles, PEG-p(Asp-Hyd-4AB-PTX) micelles, and their mixed polymeric micelles (1:1 and 1:5) were evaluated in MCF-7 and SK-OV-3 cell lines (Table 1). The IC_{50} values of PTX for MCF-7 and SK-OV-3 cell lines were 4.60 ± 1.17 and 1.84 ± 0.40 nM, respectively (Figs. 8A & 8B). The IC_{50} values for LEV-PTX for MCF-7 and SK-OV-3 cell lines were slightly higher: 11.17 ± 0.66 and 5.17 ± 2.18 nM, respectively, whereas the IC_{50} values for 4AB-PTX for MCF-7 and SK-OV-3 cell lines were 17.19 ± 1.05 and 29.02 ± 5.06 nM, respectively (Figs. 8A & 8B). The IC_{50} values for PEG-p(Asp-Hyd-LEV-PTX) micelles for MCF-7 cells and SK-OV-3 cell lines were 8.00 ± 0.614 nM and 4.43 ± 0.86 nM, respectively (Figs. 8C & 8D). The IC_{50} values for mixed polymeric micelles at 1:1 and 1:5 molar ratios for MCF-7 cells were 12.58 ± 3.25 and 9.72 ± 2.28 nM, respectively, whereas the IC_{50} values for SK-OV-3 cells were 6.21 ± 1.64 nM and 8.72 ± 0.99, respectively (Figs. 8C & 8D). PEG-p(Asp-Hyd-4AB-PTX) micelles (Table 1), PEG-p(Asp-Hyd-LEV) and PEG-p(ASP-Hyd-4AB) showed no cytotoxicity against MCF-7 and SK-OV-3 cell lines (data not shown).

4. Discussion

Polymeric micelles are gaining increasing attention in the field of anti-cancer drug delivery, owing to prospects for drug solubilization and more recently for controlled drug release, which in concert with the EPR effect could permit prolonged circulation in blood, preferential accumulation at solid tumors, and drug release, triggered by an acidic extracellular milieu often found at solid tumors or by low pH 4–5 encountered after cellular entry in the endosomes/lysosomes [17–20]. PTX lacks an aldehyde or ketone functional group for hydrazone chemistry, and ester prodrugs of PTX usually involve its C-2′-OH-position [24]. Thus, we have used an aliphatic linker, LEV or an aromatic linker 4AB, as a

spacer group on PEG-p(Asp-Hyd) (Fig. 1 and 3), gaining 100% substitution of LEV or 4AB on PEG-p(Asp-Hyd) based on ^{1}H NMR spectroscopy (Fig. 4). PTX reacts with PEG-p(Asp-Hyd-LEV) or PEG-p(Asp-Hyd-4AB) through its C-2′-OH-position by DIC/DMAP coupling, resulting in PEG-p(Asp-Hyd-LEV-PTX) and PEG-p(Asp-Hyd-4AB-PTX) (Fig. 3), with degrees of drug substitution at 37.5 and 87.5%, respectively, based on ^{1}H NMR spectroscopy (Fig. 4). It is anticipated that the degrees of PTX can be varied by using varied ratios of PTX to PEG-p(Asp-Hyd-LEV-PTX) or PEG-p(Asp-Hyd-4AB-PTX). We note that LEV-PTX and 4AB-PTX react poorly with PEG-p(Asp-Hyd), resulting in low degrees of PTX substitution (data not shown), and we have not pursed this pathway toward PEG-p(Asp-Hyd-LEV-PTX) or PEG-p(Asp-Hyd-4AB-PTX).

DLS measurements have provided evidence that PEG-p(Asp-Hyd-LEV-PTX) or PEG-p(Asp-Hyd-4AB-PTX) assembles into unimodal polymeric micelles (Fig 6.). PEG-p(Asp-Hyd-LEV-PTX) assembles into smaller polymeric micelles (41.9 ± 0.6 nm versus 137 ± 2.4 nm) than PEG-p(Asp-Hyd-4AB-PTX) micelles, reflecting a higher degree of PTX substitution, which may provide a higher association number for PEG-p(Asp-Hyd-4AB-PTX) micelles. Interestingly, a co-assembly of PEG-p(Asp-Hyd-LEV-PTX) and PEG-p(Asp-Hyd-4AB-PTX) (1:1 ratio) gives rise to unimodal polymeric micelles with an average hydrodynamic diameter of 85.53 ± 0.14 nm, which is in between the values for PEG-p(Asp-Hyd-LEV-PTX) and PEG-p(Asp-Hyd-4AB-PTX) micelles and is indicative of mixed polymeric micelles. With an increase in content of PEG-p(Asp-Hyd-4AB-PTX) (1:5), PEG-p(Asp-Hyd-LEV-PTX) and PEG-p(Asp-Hyd-4AB-PTX) assembles into larger polymeric micelles (113.40 ± 0.93 nm), which are again unimodal and indicative of mixed polymeric micelles composed of PEG-p(Asp-Hyd-LEV-PTX) and PEG-p(Asp-Hyd-4AB-PTX). PEG-p(Asp-Hyd-LEV-PTX) and PEG-p(Asp-Hyd-4AB-PTX) micelles effectively increase the water solubility of PTX, reaching mg/mL levels, which are required for cancer therapy.

PEG-p(Asp-Hyd-LEV-PTX) micelles release LEV-PTX in a pH-dependent manner *in vitro*, showing faster release at pH 5.0 than at pH 7.4 (Fig. 7). Our results suggest that PEG-p(Asp-Hyd-LEV-PTX) micelles release LEV-PTX and not PTX, indicating that the ester bond in LEV-PTX is quite stable. This result is consistent with earlier published research on a PEG prodrug of 4AB-PTX, where 4AB-PTX is the only species released at pH 4.0 [25]. Unlike this previous study, PEG-p(Asp-Hyd-4AB-PTX) micelles did not release any 4AB-PTX at pH 5.0 or 7.4.

The higher stability of PEG-p(Asp-Hyd-4AB-PTX) micelles can be attributed to the compartmentalization of 4AB-PTX in the core region of polymeric micelles. The higher stability of PEG-p(Asp-Hyd-4AB-PTX) micelles over PEG-p(Asp-Hyd-LEV-PTX) micelles can be attributed to the high stability of the 4AB (aromatic) hydrazone bond over a LEV (aliphatic) hydrazone bond and the higher number of PTX attached on PEG-p(Asp-Hyd-4AB-PTX), resulting in increased core hydrophobicity. While major differences between PEG-p(Asp-Hyd-4AB-PTX) micelles and PEG-p(Asp-Hyd-LEV-PTX) micelles emerge *in vitro*, it is expected that these differences will be less *in vivo*, where both polymeric micelles will undergo disassembly into unimers, which will be exposed to water and hydrolysis.

We have hypothesized that PEG-p(Asp-Hyd-LEV-PTX) and PEG-p(Asp-Hyd-4AB-PTX) will co-assemble into mixed polymeric micelles, affecting drug release. At a 1:1 ratio, the release of LEV-PTX is similar to the release pattern of LEV-PTX for PEG-p(Asp-Hyd-LEV-PTX) micelles (Fig. 7), noting that the total quantity of LEV-PTX was equivalent for all the samples. At a 1:5 ratio, i.e. a greater content of PEG-p(Asp-Hyd-4AB-PTX), the release of LEV-PTX is slower at pH 5.0, relative to PEG-p(Asp-Hyd-LEV-PTX) micelles, suggesting that an increase in core hydrophobicity by PEG-p(Asp-Hyd-4AB-PTX) by co-assembly slows drug release. Thus, the ratio of the LEV-PTX to 4AB-PTX can be altered in mixed polymeric micelles, resulting in a moderation of drug release under acidic conditions.

Across the board, IC_{50} values for PTX and all its analogs are comparable for MCF-7 and SK-OV-3 cancer cell lines (Figs. 8A & 8B), even for mixed polymeric micelles at a 1:5 ratio (Table 1). These results indicate that LEV-PTX that is gradually released from PEG-p(Asp-Hyd-LEV-PTX) micelles and its mixed polymeric micelles results in the growth inhibition or apoptosis of cancer cells. Apoptotic assays will show whether cancer cell killing changes as a result of pH-dependent release for PEG-p(Asp-Hyd-LEV-PTX) micelles and its mixed polymeric micelles. Similarly, it will be interesting to study whether the anti-angiogenesis activity of PTX has been moderated. Interestingly, cytotoxicity for LEV-PTX, 4AB-PTX, PEG-p(Asp-Hyd-LEV-PTX) micelles, and PEG-p(Asp-Hyd-4AB-PTX) mixed polymeric micelles indicates that LEV-PTX and 4AB-PTX undergo hydrolysis in cell culture, probably due to the action of esterases in FBS. Previous studies have shown that the hydroxyl group at the 2′-position of PTX (Fig. 2) is required for cytotoxicity [24, 26].

Current commercial and new PTX formulations focus on exploiting its mitotic inhibitory effect, which requires maximum tolerated doses of PTX to be delivered on a rotating schedule. The new paradigm shift in cancer therapy has indicated that PTX at low doses can be a potent anti-angiogenic agent. Thus, the focus of our work and the proof of concept experiments conducted by our lab are looking to produce PTX formulations that will highlight its anti-angiogenic effects which can be augmented by administering comparatively low doses of PTX over. Traditional polymer chemistry would accomplish this by creating a library of polymers with different number of PTX attached to the backbone. Our system allows us to minimize the synthesis needed to two set of polymer constructs. By mixing these polymers constructs in different ratios to form polymeric micelles we can achieve controlled release of PTX under acidic conditions. Thus, enabling us to elegantly tailor concentration of PTX under specified set of conditions. Further studies are planned to test the *in vivo* efficacy of these systems in mice tumor models to further validate this approach. The ultimate advantage of successfully implementing this kind of a formulation will allow patients to have continuous therapy with much lower side effects leading to higher patient compliance rates and better quality of life.

5. Conclusions

We have synthesized two micelle-forming prodrugs of PTX: PEG-p(Asp-Hyd-LEV-PTX) and PEG-p(Asp-Hyd-4AB-PTX). Both ABCs assemble into polymeric micelles that can increase the water solubility of PTX. PEG-p(Asp-Hyd-LEV-PTX) micelles release LEV-PTX in a pH-dependent manner. PEG-p(Asp-Hyd-LEV-PTX) and PEG-p(Asp-Hyd-4AB-

PTX) co-assemble into mixed polymeric micelles that moderate the release of LEV-PTX relative to PEG-p(Asp-Hyd-LEV-PTX) micelles, owing to the hydrophobicity of PEG-p(Asp-Hyd-4AB-PTX). Thus, release of PTX can be moderated by choice of linker (4AB versus LEV) and assembly into mixed polymeric micelles. This system can be easily adapted to facilitate the control of the PTX release by simply controlling the mixing ratio of the of PEG-p(Asp-Hyd-LEV-PTX) and PEG-p(Asp-Hyd-4AB-PTX) in the mixed polymeric micelles, Cytotoxicity experiments suggest that all analogues of PTX retain cell growth inhibitory activity against MCF-7 and SK-OV-3 cancer cells, indicating hydrolysis of the ester bond in LEV-PTX and 4AB-PTX. PEG-p(Asp-Hyd-LEV-PTX) micelles, PEG-p(Asp-Hyd-4AB-PTX) micelles, or their mixed polymeric micelles have unique potential for the delivery of PTX, owing to prospects for prolonged circulation in blood, high tumor accumulation by the EPR effect, and pH-dependent release, enabling flexibility in the action of PTX against cancer cells and anti-angiogenesis activity.

References

1. McGuire, WP.; Rowinsky, EK. Paclitaxel in cancer treatment. New York: M. Dekker; 1995.
2. Ng SSW, Sparreboom A, Shaked Y, Lee C, Man S, Desai N, et al. Influence of formulation vehicle on Metronomic taxane chemotherapy: Albumin-bound versus Cremophor EL® based paclitaxel. Clin Cancer Res. 2006; 12(14):4331–4338. [PubMed: 16857808]
3. Ng SSW, Figg WD, Sparreboom A. Taxane-mediated antiangiogenesis *in vitro*: influence of formulation vehicles and binding proteins. Cancer Res. 2004; 64(3):821–824. [PubMed: 14871806]
4. Belotti D, Rieppi M, Nicoletti MI, Casazza AM, Fojo T, Taraboletti G, et al. Paclitaxel (Taxol(R)) inhibits motility of paclitaxel-resistant human ovarian carcinoma cells. Clin Cancer Res. 1996; 2(10):1725–1730. [PubMed: 9816123]
5. Kerbel RS, Kamen BA. The anti-angiogenic basis of metronomic chemotherapy. Nat Rev Cancer. 2004; 4(6):423–436. [PubMed: 15170445]
6. Lee SC, Huh KM, Lee J, Cho YW, Galinsky RE, Park K. Hydrotropic Polymeric Micelles for Enhanced Paclitaxel Solubility: In Vitro and In Vivo Characterization. Biomacromolecules. 2007; 8(1):202–208. [PubMed: 17206808]
7. Weiss R, Donehower R, Wiernik P, Ohnuma T, Gralla R, Trump D, et al. Hypersensitivity reactions from taxol. J Clin Oncol. 1990; 8(7):1263–1268. [PubMed: 1972736]
8. Lorenz W, Reimann H-J, Schmal A, Dormann P, Schwarz B, Neugebauer E, et al. Histamine release in dogs by Cremophor EL ® and its derivatives: Oxethylated oleic acid is the most effective constituent. Inflammation Research. 1977; 7(1):63–67.
9. Dye D, Watkins J. Suspected anaphylactic reaction to Cremophor EL. British Medical Journal. 1980; 280(6628):1353. [PubMed: 7388538]
10. Waugh WN, Trissel LA, Stella VJ. Stability, compatibility, and plasticizer extraction of taxol (NSC-125973) injection diluted in infusion solutions and stored in various containers. American Journal of Hospital Pharmacy. 1991; 48(7):1520–1524. [PubMed: 1679294]
11. Allwood MC, Martin H. The extraction of diethylhexylphthalate (DEHP) from polyvinyl chloride components of intravenous infusion containers and administration sets by paclitaxel injection. International Journal of Pharmaceutics. 1996; 127(1):65–71.
12. Hawkins MJ, Soon-Shiong P, Desai N. Protein nanoparticles as drug carriers in clinical medicine. Advanced Drug Delivery Reviews. 2008; 60(8):876–885. [PubMed: 18423779]
13. Matsumura Y, Maeda H. A new foccept for macromolecular therapeutics in cancer chemotherapy: Mechanism of tumoritropic accumulation of proteins and the antitumor agent smancs. Cancer Res. 1986; 46(12_Part_1):6387–6392. [PubMed: 2946403]
14. Yokoyama M, Miyauchi M, Yamada N, Okano T, Sakurai Y, Kataoka K, et al. Characterization and anticancer activity of the micelle-forming polymeric anticancer drug adriamycin-conjugated

poly(ethylene glycol)-poly(aspartic acid) block copolymer. Cancer Res. 1990; 50(6):1693–1700. [PubMed: 2306723]

15. Yokoyama M, Mizue M, Noriko Y, Teruo O, Yasuhisa S, Kazunori K, et al. Polymer micelles as novel drug carrier: Adriamycin-conjugated poly(ethylene glycol)-poly(aspartic acid) block copolymer. Journal of Controlled Release. 1990; 11(1–3):269–278.
16. Matsumura Y. Poly (amino acid) micelle nanocarriers in preclinical and clinical studies. Advanced Drug Delivery Reviews. 2008; 60(8):899–914. [PubMed: 18406004]
17. Bae Y, Diezi TA, Zhao A, Kwon GS. Mixed polymeric micelles for combination cancer chemotherapy through the concurrent delivery of multiple chemotherapeutic agents. Journal of Controlled Release. 2007; 122(3):324–330. [PubMed: 17669540]
18. Bae Y, Fukushima S, Harada A, Kataoka K. Design of environment-sensitive Supramolecular assemblies for intracellular drug delivery: Polymeric micelles that are responsive to intracellular pH change. Angewandte Chemie International Edition. 2003; 42(38):4640–4643.
19. Bae Y, Jang W-D, Nishiyama N, Fukushima S, Kataoka K. Multifunctional polymeric micelles with folate-mediated cancer cell targeting and pH-triggered drug releasing properties for active intracellular drug delivery. Molecular BioSystems. 2005; 1(3):242–250. [PubMed: 16880988]
20. Bae Y, Nishiyama N, Kataoka K. *In vivo* antitumor activity of the folate-conjugated pH-sensitive polymeric micelle selectively releasing adriamycin in the intracellular acidic compartments. Bioconjugate Chem. 2007; 18(4):1131–1139.
21. Yokoyama M, Kwon GS, Okano T, Sakurai Y, Seto T, Kataoka K. Preparation of micelle-forming polymer-drug conjugates. Bioconjugate Chemistry. 1992; 3(4):295–301. [PubMed: 1390984]
22. Yokoyama M, Okano T, Sakurai Y, Kataoka K. Improved synthesis of adriamycin-conjugated poly (ethylene oxide)-poly (aspartic acid) block copolymer and formation of unimodal micellar structure with controlled amount of physically entrapped adriamycin. Journal of Controlled Release. 1994; 32(3):269–277.
23. Solutions. United States Pharmacopeia and National Formulary (USP 24-NF 19). Rockville, MD: The United States Pharmacopeia Convention, Inc; 2000. p. 2231-2247.
24. Mellado W, Magri NF, Kingston DGI, Garcia-Arenas R, Orr GA, Horwitz SB. Preparation and biological activity of taxol acetates. Biochemical and Biophysical Research Communications. 1984; 124(2):329–336. [PubMed: 6548627]
25. Rodrigues PCA, Scheuermann K, Stockmar C, Maier G, Fiebig HH, Unger C, et al. Synthesis and In vitro efficacy of acid-Sensitive poly(ethylene glycol) paclitaxel conjugates. Bioorganic & Medicinal Chemistry Letters. 2003; 13(3):355–360. [PubMed: 12882225]
26. Mathew AE, Mejillano MR, Nath JP, Himes RH, Stella VJ. Synthesis and evaluation of some water-soluble prodrugs and derivatives of taxol with antitumor activity. Journal of Medicinal Chemistry. 1992; 35(1):145–151. [PubMed: 1346275]

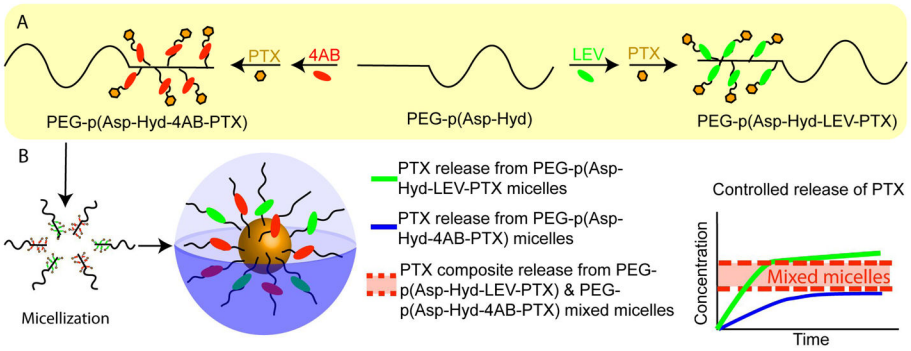

Fig. 1.

Synthesis scheme for PEG-p(Asp-Hyd-LEV-PTX) and PEG-p(Asp-Hyd-4AB-PTX) (A); A sketch of a mixed polymeric micelle and expected PTX release profiles from PEG-p(Asp-Hyd-LEV-PTX), PEG-p(Asp-Hyd-4AB-PTX) micelles and mixed polymeric micelles (B)

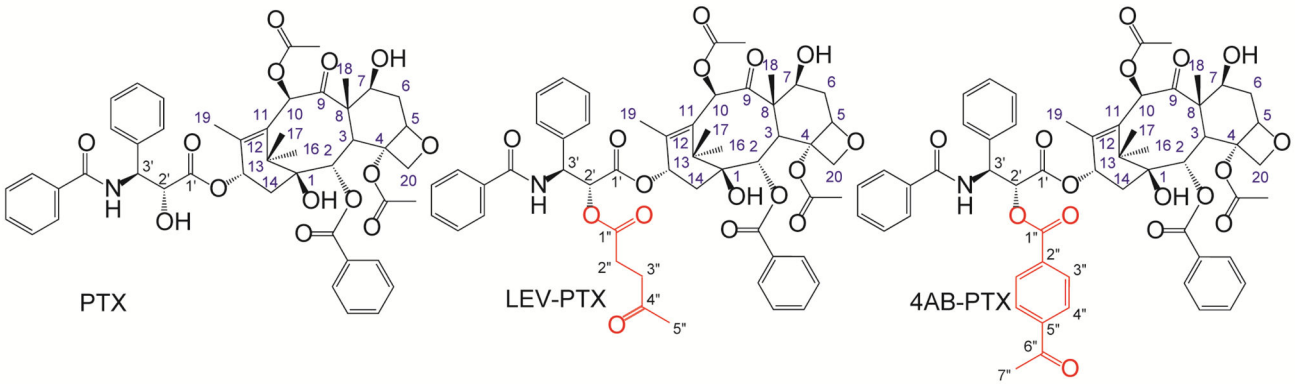

Fig. 2.

Chemical structures of LEV-PTX and 4AB-PTX as confirmed by ^{1}H NMR, ^{13}C NMR, 2D HSQC (Heteronuclear Single Quantum Coherence) and reverse-phase HPLC.

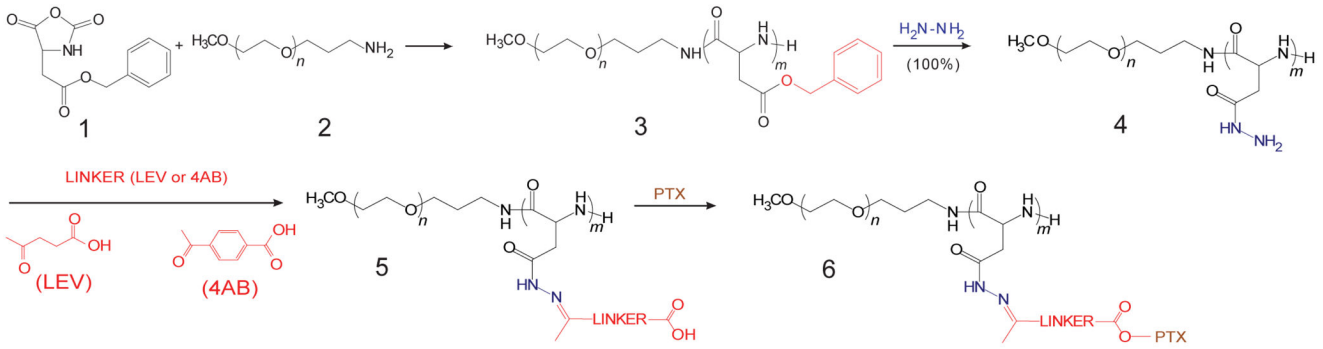

Fig. 3.
Synthesis scheme of PEG-p(Asp-Hyd-4AB-PTX) or PEG-p(Asp-Hyd-LEV-PTX)

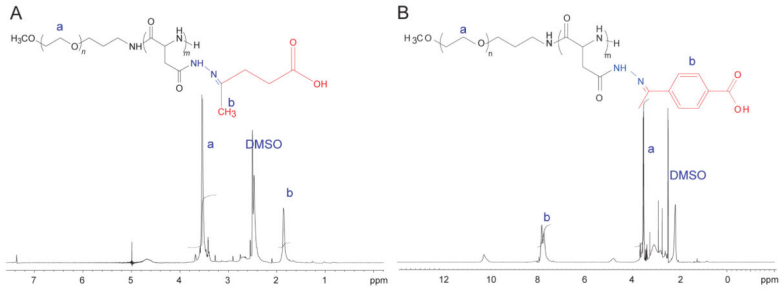

Fig. 4.

^{1}H NMR spectra of PEG-p(Asp-Hyd-LEV) (A) and PEG-p(ASP-Hyd-4AB) (B). NMR measurements were performed on ^{UNITY}*INOVA* NMR spectrometers (Varian, USA) model operating at 500 MHz in DMSO-d_6 and at 80 °C.

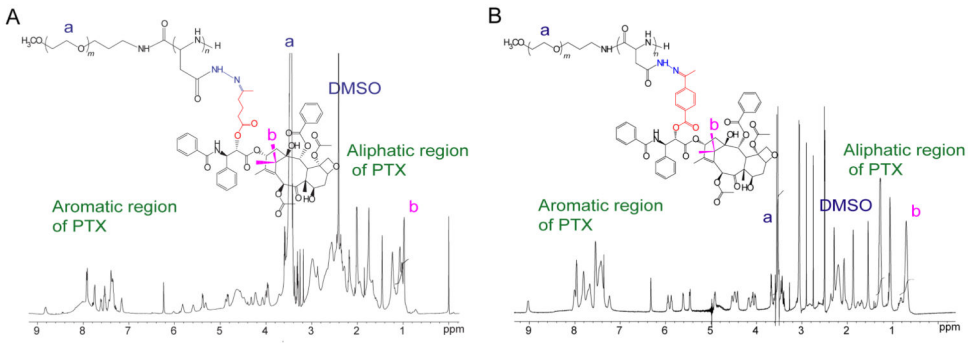

Fig. 5.

^{1}H NMR spectra of PEG-p(Asp-Hyd-LEV-PTX) (A) and PEG-p(ASP-Hyd-4AB-PTX) (B). NMR measurements were performed on $^{\text{UNITY}}$*INOVA* NMR spectrometers (Varian, USA) model operating at 500 MHz in DMSO-d_6 and at 80 °C.

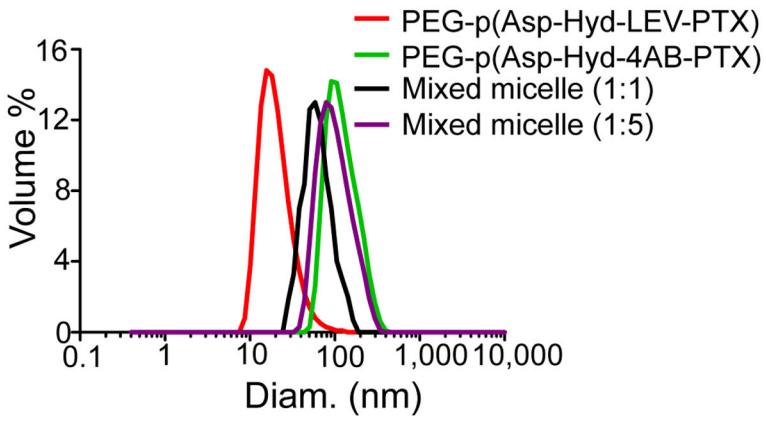

Fig. 6.

Particle size distributions (volume-weighted) for PEG-p(Asp-Hyd-LEV-PTX) micelles, PEG-p(Asp-Hyd-4AB-PTX) micelles, and their mixed polymeric micelles (1:1 and 1:5).

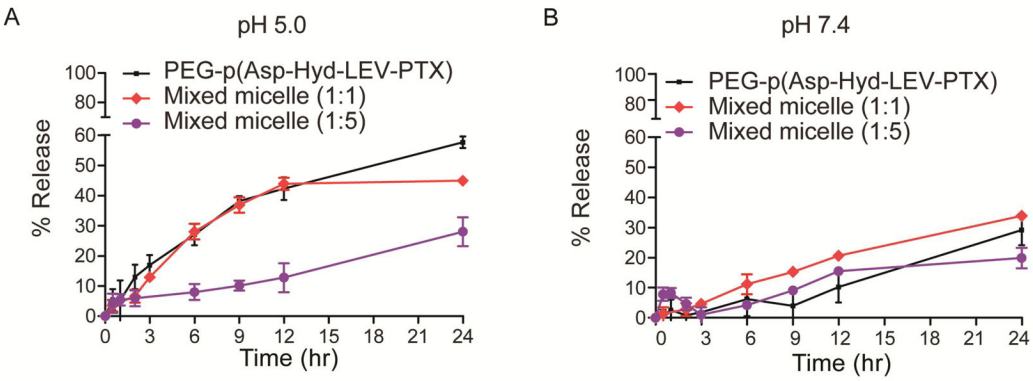

Fig. 7.

In vitro release profiles of LEV-PTX from PEG-p(Asp-Hyd-LEV-PTX), mixed polymeric micelles (1:1 molar ratio), or mixed polymeric micelles (1:5 molar ratio) at pH 5.0 (A) and pH 7.4 (B). No 4AB-PTX was significantly released from PEG-p(Asp-Hyd-4AB-PTX) micelles or mixed polymeric micelles. (Mean ± SD, n=3)

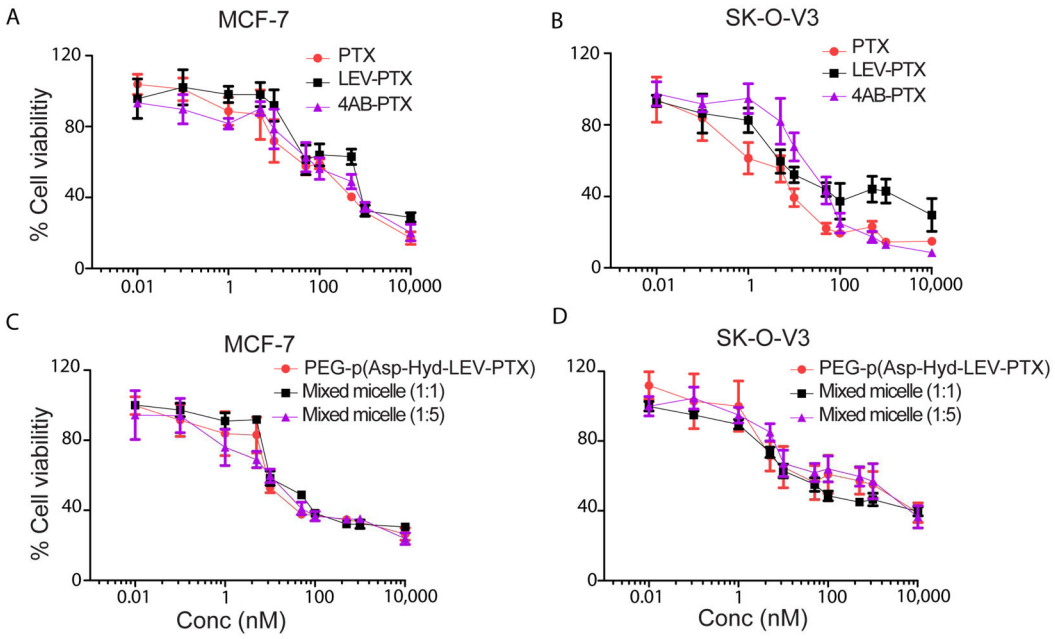

Fig. 8.

MCF-7 (human breast adenocarcinoma) and SK-OV-3 (human caucasian ovary adenocarcinoma) cell lines viability compared to control (untreated cells). Cells were treated with PTX, LEV-PTX, or 4AB-PTX (A and B). Cells were treated with PEG-p(Asp-Hyd-LEV-PTX) micelles, mixed polymeric micelles 1:1 or 1:5 molar ratios (C and D). (Mean ± SD, n=4)

Table 1

PTX, LEV-PTX, 4AB-PTX, individual and mixed polymeric micelles cytotoxicity in MCF-7 and SK-OV-3 human cell lines. Cells were incubated with the each formulation for 72hr thereafter cell viability was assessed by CellTiter-Blue® Cell Viability Assay.

Formulation	[a] **IC_{50} (nM) (Mean ± SD)**	
	MCF-7	**SK-OV-3**
PTX	4.60 ± 1.17	1.84 ± 0.40
LEV-PTX	11.17 ± 0.66	5.17 ± 2.18
4AB-PTX	17.19 ± 1.05	29.02 ± 5.06
PEG-p(Asp-Hyd-LEV-PTX) (individual micelle)	8.00 ± 0.614	4.43 ± 0.86
PEG-p(Asp-Hyd-4AB-PTX) (individual micelle)	---	---
Mixed Micelle 1:1	12.58 ± 3.25	6.21 ± 1.64
Mixed Micelle 1:5	9.72 ± 2.28	8.72 ± 0.99

[a] IC_{50} was calculated by fitting the data to log(inhibitor) vs. response -Variable slope equation using GraphPad Prism version 5.00 for Windows. (Mean ± SD, n=3)